



Microstructural and Thermal Characterization of Aluminum Bronzes

Z.Ezel DOĞAN¹, Fulya KAHRIMAN¹, Ş. Hakan ATAPEK^{1,*}

¹Metallurgical and Materials Engineering, Kocaeli University, Kocaeli, 41380, Turkey

Article Info

Research paper

Received : 14/03/2018

Accepted : 15/05/2018

Keywords

Aluminum bronze
Solidification
Microstructure
Characterization

Abstract

In this study, microstructures and the solidification characteristics of heat treatable Cu-Al-Fe-Ni based alloys were investigated. Initial microstructural features of conventional alloys were examined by microscopical analysis and not only the martensitic structure but also several kappa phases embedded in copper based matrix were observed. Then, thermal analysis was performed in order to reveal the solidification sequence under cooling and the findings on the crystallization were in good agreement with the data reported earlier.

1. Introduction

Aluminum bronzes, especially nickel-aluminum ones, are widely used in chemical plants, marine parts, aviation and bearing systems due to their high strength, corrosion and wear resistance. These alloys are heat treatable alloys and contain 8-14 % Al, 2-4 % Mn, Ni and Fe. Their microstructural features vary as a function of both casting process and heat treatment procedures. By casting, a typical nickel-aluminum bronze solidifies at the temperature around 1070 °C and the alloy has a great diversity of microstructural features during slow cooling to room temperature. By heat treatment procedure consisting of solution annealing, quenching and tempering, a tempered martensitic/bainitic microstructure could be achieved and these structures enhance the mechanical properties of the nickel-aluminum bronzes [1-5].

According to Cu-Al equilibrium diagram [6], the structure of aluminum bronze consists of α -phase, β -phase, γ -phase and several electronic compounds (Cu₃Al, Cu₃₂Al₁₉ etc.), however, many alloying elements (Fe, Mn and Ni) are responsible for the formation of several precipitates known as kappa phases. The mechanical properties are also affected by these precipitates [7-10].

The type and amount of these precipitates could be changed as a function of the applied heat treatment routes. In the re-design of the bronze matrix, both solution annealing and tempering temperature play an important role and all exothermic/endothermic reactions related to the phase transformation can be investigated.

In this study, two commercial nickel-aluminum bronzes having different iron and manganese content were provided and their both microstructural features and solidification characteristics were characterized by metallurgical and thermal analysis. The results showed that the amount of iron and manganese are very effective on the type and amount of kappa precipitates and also on the solidification path of the studied alloys.

2. Materials and Methods

Cast and forged Cu-9Al-3Fe-5Ni-1Mn and Cu-10Al-4.8Fe-5Ni-1.5Mn alloys were provided from Sağlam Metal Co. The characterization studies were carried out in two stages; (i) microstructural characterization and (ii) thermal analysis. In microstructural characterization, samples were prepared by metallographically. The samples were ground with 320, 600, and 1000 mesh size SiC

* Corresponding Author: hatapek@kocaeli.edu.tr

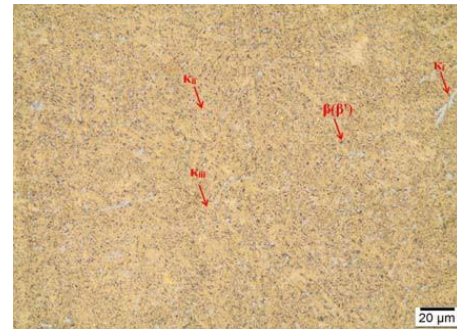
abrasives, and then polished with 3 μm diamond solution. Polished surface was etched by a solution including 50 ml HCl, 10 ml HNO_3 , 10 g FeCl, 100 ml H_2O . Microstructural characterization was carried out using light microscope (LM, Olympus BX41M-LED) and scanning electron microscope (SEM, Jeol JSM 6060). In order to determine solidification characteristics of the studied alloys, thermal analysis was conducted. The thermal analysis were carried out by using differential thermal analysis (DTA) and differential scanning calorimeter (DSC) method on Netzsch STA 409 PG Luxx. The samples were heated to 1100 $^\circ\text{C}$ with a heating rate of 5 $\text{K}\cdot\text{min}^{-1}$, held at that temperature for 5 min, and then cooled to room temperature (RT) with a rate of 5 $\text{K}\cdot\text{min}^{-1}$.

3. Results and Discussion

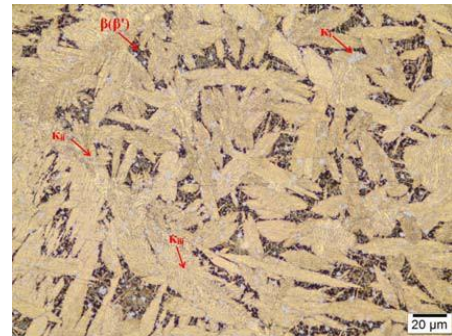
3.1. Microstructural characterization

As reported in previous studies for a solidified nickel-aluminum bronze [11, 12], the microstructure consists entirely of β -phase until the alloy is cooled down below 1030 $^\circ\text{C}$ and α -phase forms within β -phase. About 930 $^\circ\text{C}$, a globular intermetallic phase (κ_{ii}) begins to form within β -phase and a coarser intermetallic phase (κ_i) is appears within the β -phase due to higher iron content. When the temperature falls down to 860 $^\circ\text{C}$, another intermetallic phase (κ_{iv}) starts to form within α -phase as a function of iron content. At 800 $^\circ\text{C}$, due to the eutectoid reaction, the remaining β -phase is transformed to the intermetallic κ_{iv} phase. In fact, it is expected that the solidified structure consists of several kappa phases embedded in α -phase, however, if the cooling rate is higher, some β -phase remains and the matrix includes β' -phase known as retained β -phase.

Figure 1 shows the microstructures of studied alloys and all microstructural features within alloy matrices are introduced. Generally the microstructure consists of grains of α phase (fcc copper-rich solid solution), a small volume fraction of $\beta(\beta')$ phase (solid solution with martensitic structure) and intermetallic κ phases. The κ_i phases appears as the rosette-like precipitates and these precipitates are based on Fe_3Al . The dendritic-shaped precipitates are κ_{ii} phases; they are not only distributed at the α/β boundaries but also smaller than κ_i . The matrices have lamellar or globular eutectoidal decomposition products known as Ni-rich (NiAl) κ_{iii} phases. The Fe-rich κ_{iv} phases are very fine particles and they are visible within the high resolution SEM image given in Figure 2. The elemental distribution was also studied and the micrographs given in Figure 3 shows the Al, Fe and Ni-rich kappa phases embedded in copper based matrix.

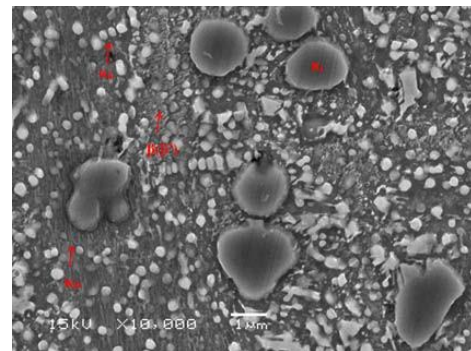


(a)

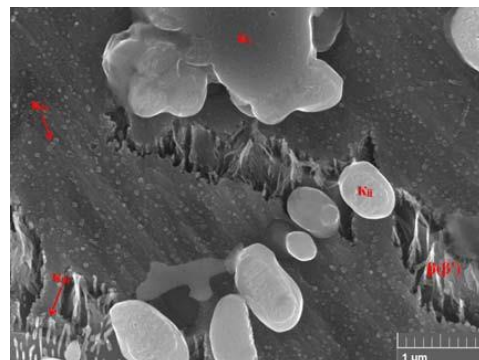


(b)

Figure 1. LM images showing the matrices of studied alloys; (a) Cu-9Al-3Fe-5Ni-1Mn and (b) Cu-10Al-4.8Fe-5Ni-1.5Mn.



(a)



(b)

Figure 2. SEM images showing the obtained phases Cu-9Al-3Fe-5Ni-1Mn (a) and Cu-10Al-4.8Fe-5Ni-1.5Mn (b).

3.2. Thermal characterization

The solidification sequences of each alloy were determined by both DTA and DSC analysis and the obtained thermograms are given in Figure 3. In thermograms, several phase transformations were observed. In the Cu-Al-Fe-Ni system the following six reactions could be observed by TDA (Thermal Derivative Analysis) and these reactions include not only liquid-solid/solid-solid phase transformations but also precipitation reactions; (i) β crystallization from liquid, (ii) both κ_i and κ_{ii} precipitation within β -phase, (iii) α crystallization from β -phase, (iv) κ_{iii} precipitation within α -phase, (v) κ_{iv} precipitation within α -phase and (vi) eutectoid transformation ($\beta \rightarrow \alpha + \gamma_2$) [13]. However, no exothermic data on the precipitation of κ phases was determined in both DTA and DSC analysis.

In the Cu-Al-Fe-Ni system, β -phase was crystallized from liquid and both liquidus and solidus temperature was affected by the alloying elements, especially Al, Fe etc. The data obtained from thermal analyzes showed that the alloy having higher Al, Fe and Mn (Cu-10Al-4.8Fe-5Ni-1.5Mn) had an expanded solidification range, since the curves shifted to higher liquidus and solidus temperatures. The thermograms have no information on the crystallization of κ_i and κ_{ii} precipitation. Brezina [14] had studied on the crystallization of Cu-10Al-5Fe-5Ni and did not also explain clearly the stage of formation of κ_i phases. These phases preferably form in the grain boundaries of β -phase and the possibility of crystallization is affected by the portion of iron-rich liquid. Although no data on the exothermic reaction for κ_{ii} precipitation was obtained, Pisarek studied on the model of Cu-Al-Fe-Ni bronze crystallization and reported that κ_{ii} precipitates within β -phase at 897 °C [13]. In the studied system, there is a well-known solid-solid reaction and α -phase forms from β -phase. According to the thermograms given in Figure 4, α -phase crystallization in the alloy having higher Al, Fe and Mn content (Cu-10Al-4.8Fe-5Ni-1.5Mn) started within the range of 810-812 °C and the obtained data were in good agreement with the reported data in Ref. 14, since DTA studies revealed that the temperature of α -phase crystallization was 812 °C for Cu-Al-Fe-Ni system.

As mentioned before, the κ_{iii} precipitation could be accompanied with the formation of α -phase and the crystallization range of 715-800 °C is attributed to

formation of κ_{iii} phase for the studied alloys. On the other hand, the thermograms also point out the eutectoid transformation and DTA analysis showed that this transformation started at 502 °C and 522 °C for Cu-9Al-3Fe-5Ni-1Mn and Cu-10Al-4.8Fe-5Ni-1.5Mn alloys, respectively. In DSC analysis, these temperatures were obtained as 500 °C and 513 °C for Cu-9Al-3Fe-5Ni-1Mn and Cu-10Al-4.8Fe-5Ni-1.5Mn alloys, respectively.

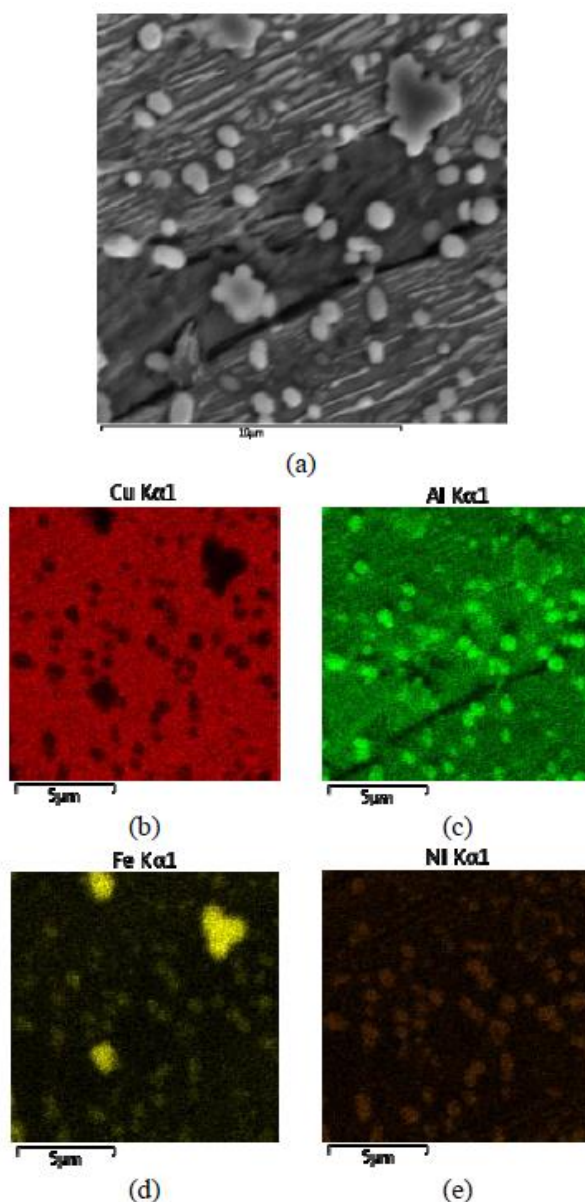


Figure 3. SEM images showing the elemental distribution of kappa phases embedded in α -Cu matrix of Cu-10Al-4.8Fe-5Ni-1.5Mn (a), the distribution of Cu (b), Al (c), Fe (d) and Ni atoms (e)

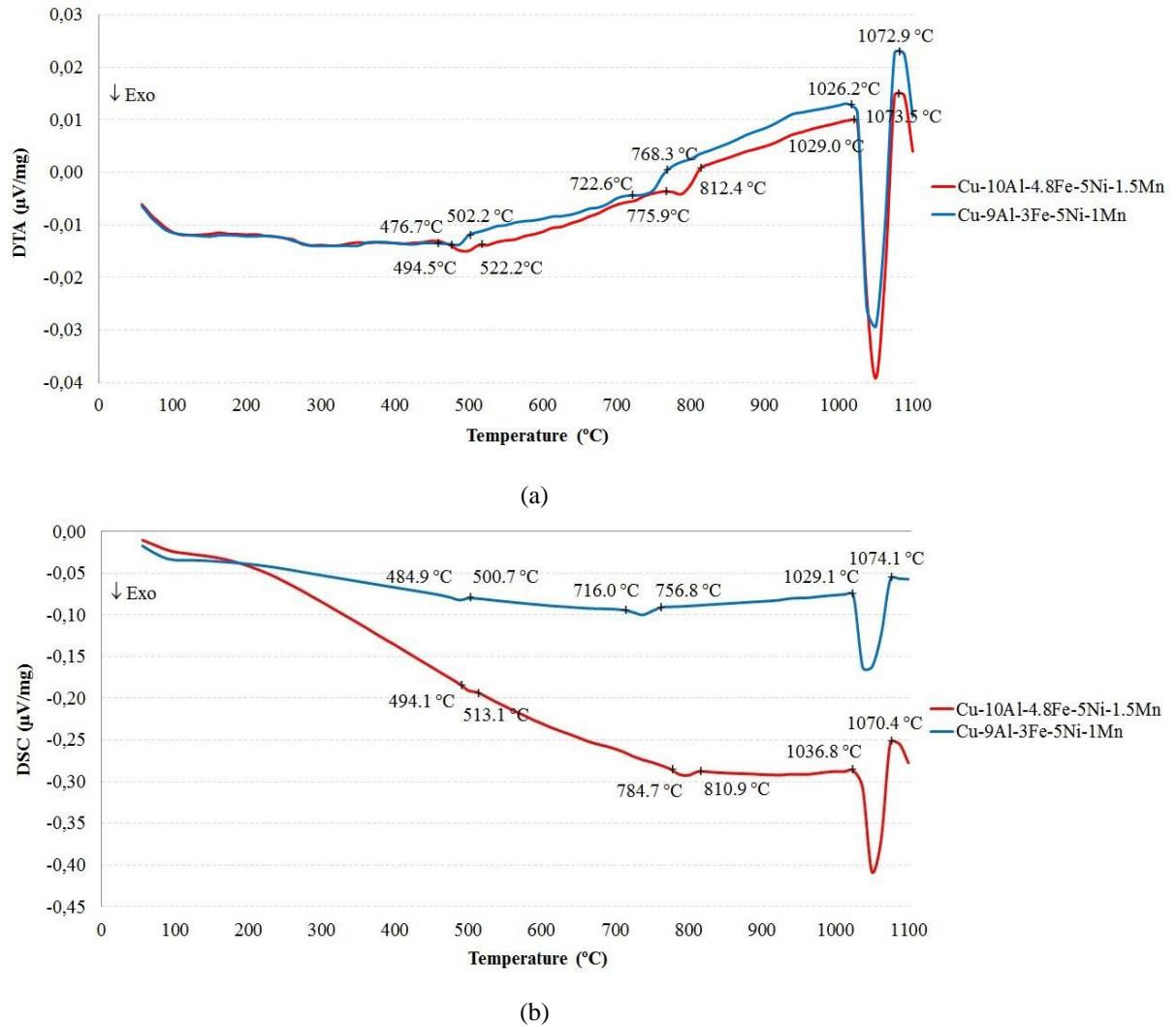


Figure 4. Thermograms showing the solidification sequence of the studied alloys; (a) DTA and (b) DSC.

4. Conclusions

In this study, both microstructural and thermal characterizations of two conventional Al-bronzes were investigated and the following results were obtained;

(i) The alloys had similar microstructural features and their matrices consisted of $\beta(\beta')$ and several kappa phases embedded in α -Cu. Although no morphological changes on kappa phases were observed, the amounts of these phases were varied as a function of the chemical composition of the studied alloy.

(ii) The solidification sequences of the alloys were also studied and the obtained data was in good agreement with the ones reported earlier [13, 14] and higher Al, Fe and Mn content caused a shift on the curves, thus all liquid-solid/solid-solid reactions started at higher temperatures.

References

[1] Kaplan M., Yildiz A. K., 2003. The effects of

production methods on the microstructures and mechanical properties of an aluminum bronze. *Materials Letters* **57**, 4402-4411.

[2] Anantapong J., Uthaisangsuk V., Suranuntchai S., Manonukul A., 2014. Effect of hot working on microstructure evolution of as-cast nickel aluminum bronze alloy. *Materials and Design* **60**, 233-243.

[3] Wu Z., Cheng Y. F., Liu L., Lv W., Hu W., 2015. Effect of heat treatment on microstructure evolution and erosion-corrosion behavior of a nickel-aluminum bronze alloy in chloride solution. *Corrosion Science* **98**, 260-270.

[4] Li W. S., Wang Z. P., Lu Y., Jin Y. H., Yuan L. H., Wang F., 2006. Mechanical and tribological properties of a novel aluminum bronze material for drawing dies. *Wear* **261**, 155-163.

[5] Chen R. P., Linag Z. Q., Zhang W. W., Zhang D. T., Luo Z. Q., Li Y. Y., 2007. Effect of heat treatment on microstructure and properties of hot-extruded nickel-aluminum bronze. *Transactions of Nonferrous Metals*

Society of China **17**, 1254-1258.

[6] Copper Development Association, 1992. Equilibrium diagrams, selected copper alloy diagrams illustrating the major types of phase transformation, CDA Publication No 94.

[7] Al-Hashem A., Riad W., 2002. The role of microstructure of nickel-aluminium-bronze alloy on its cavitation corrosion behavior in natural seawater. *Materials Characterization* **48**, 37-41.

[8] Lv Y., Wang L., Han Y., Xu X., Lu W., 2015. Investigation of microstructure and mechanical properties of hot worked NiAl bronze alloy with different deformation degree. *Materials Science & Engineering A* **643**, 17-24.

[9] Xu X., Lv Y., Hu M., Xiong D., Zhang L., Wang L., Lu W., 2016. Influence of second phases on fatigue crack growth behavior of nickel aluminum bronze. *International Journal of Fatigue* **82**, 579-587.

[10] Fonlupt S., Bayle B., Delafosse D., Heuze J.L., 2005. Role of second phases in the stress corrosion cracking of a nickel-aluminum bronze in saline water. *Corrosion Science* **47**, 2792-2806.

[11] Feest E. A., Cook I. A., 2013. Pre-primary phase formation in solidification of nickel-aluminium bronze. *Journal of Metals Technology* **10**, 121-124.

[12] Cenoz I., 2010. Metallography of aluminium bronze alloy as cast in permanent iron die. Association of Metallurgical Engineers of Serbia, AMES **16**, 115-122.

[13] Pisarek B. P., 2013. Model of Cu-Al-Fe-Ni bronze crystallization. *Archives of Foundry Engineering* **13**, 72-79.

[14] Brezina P., 1973. Gefügeumwandlungen und mechanische eigenschaften der mehr- aluminiumbronzen vom typ CuAl10Fe5Ni5. *Giesserei-Forschung* **25**, 1-10.